Title: Right coronary artery flow velocity and volume assessment with spiral K-space sampled breathhold velocity-encoded MRI at 3 tesla: accuracy and reproducibility.

Authors: Brandts A, Roes SD, Doornbos J, Weiss RG, de Roos A, Stuber M, Westenberg JJ

Journal: Journal of magnetic resonance imaging : JMRI

Year: 2010 May

Volume: 31

Issue: 5

Pages: 1215-23

DOI: 10.1002/jmri.22144

Published in final edited form as:
J Magn Reson Imaging. 2010 May ; 31(5): 1215–1223. doi:10.1002/jmri.22144.

Right Coronary Artery Flow Velocity and Volume Assessment with Spiral K-Space Sampled Breath-Hold Velocity-Encoded Magnetic Resonance Imaging at 3Tesla: Accuracy and Reproducibility

Anne Brandts, MD[1,*], **Stijntje D. Roes, MD**[1,*], **Joost Doornbos, PhD**[1], **Robert G. Weiss, MD**[2,3], **Albert de Roos, MD, PhD**[1], **Matthias Stuber, PhD**[2,3,4,5], and **Jos J.M. Westenberg, PhD**[1]

[1] Department of Radiology, Leiden University Medical Center, Leiden, the Netherlands [2] Department of Radiology, Johns Hopkins University, Baltimore, Maryland, USA [3] Department of Medicine, Cardiology Division, Johns Hopkins University, Baltimore, Maryland, USA [4] Department of Electrical and Computer Engineering, Division of MR Research, Johns Hopkins University, Baltimore, Maryland, USA [5] Department of Radiology, Centre Hospitalier Universitaire Vaudois and University of Lausanne, Lausanne, Switzerland

Abstract

Purpose—To evaluate accuracy and reproducibility of flow velocity and volume measurements in a phantom and in human coronary arteries using breath-hold velocity-encoded (VE) MRI with spiral k-space sampling at 3Tesla.

Materials and Methods—Flow velocity assessment was performed using VE MRI with spiral k-space sampling. Accuracy of VE MRI was tested *in vitro* at five constant flow rates. Reproducibility was investigated in 19 healthy subjects (mean age 25.4± 1.2 years, 11 men,) by repeated acquisition in the right coronary artery (RCA).

Results—MRI-measured flow rates correlated strongly with volumetric collection (Pearson correlation r=0.99; p<0.01). Due to limited sample resolution, VE MRI overestimated the flow rate by 47% on average when non-constricted region-of-interest segmentation was used. Using constricted region-of-interest segmentation with lumen size equal to ground-truth luminal size, less than 13% error in flow rate was found. *In vivo* RCA flow velocity assessment was successful in 82% of the applied studies. High interscan, intra- and inter-observer agreement was found for almost all indices describing coronary flow velocity. Reproducibility for repeated acquisitions varied by less than 16% for peak velocity values and by less than 24% for flow volumes.

Conclusion—3T breath-hold VE MRI with spiral k-space sampling enables accurate and reproducible assessment of RCA flow velocity.

Keywords

Accuracy – Reproducibility; MRI; Coronary flow velocity

Corresponding author: Jos J.M. Westenberg, PhD, Telephone number: +31-71-5262993, Fax: +31-71-5248256, j.j.m.westenberg@lumc.nl, Department of Radiology, Leiden University Medical Center, Albinusdreef 2, PO Box 9600, 2300 RC Leiden, The Netherlands.

*Brandts and Roes both contributed equally to study design, analysis and article, therefore shared first authorship is proposed.

INTRODUCTION

The identification of luminal coronary artery disease is of high interest as this is an important risk factor for the development of ischemic cardiovascular events (1). The hemodynamic significance of coronary artery stenoses can be evaluated by measuring changes in blood-flow velocity indices and fractional flow reserve (2–4). Velocity-encoded (VE) Magnetic Resonance Imaging (MRI) has been used to estimate coronary blood flow using various field strengths and imaging sequences (4).

However, MRI coronary flow assessment remains challenging for various reasons. First, a high spatial resolution is mandatory to accurately assess the blood flow in small diameter vessels such as the coronary arteries (5). Second, in order to study the pulsatility of the flow velocity pattern, adequate temporal resolution is mandatory. Third, VE data must be obtained rapidly within a narrow acquisition window in order to minimize cardiac motion artifacts (5).

High-field 3T MRI enables image acquisition with submillimeter spatial resolution (6). Johnson et al. recently demonstrated that VE MRI at 3T using a fast low-angle shot (FLASH) sequence is an accurate tool for non-invasive *in vitro* flow velocity measurement in small diameter tubes (5). Keegan et al. demonstrated that 1.5T spiral MRI more accurately estimated coronary flow velocities throughout the cardiac cycle as compared to 1.5T FLASH MRI, particularly in the right coronary artery (RCA) (7). Furthermore, interleaved spiral k-space sampling enables rapid data collection within a breath-hold with sufficient signal-to-noise and spatial resolution for VE MRI of the coronary arteries (8) and sufficient temporal resolution for studying flow velocity waveforms (9).

However, studies on coronary flow velocity and volume using VE MRI with fast spiral k-space sampling at 3T have not been published and validation of accuracy and reproducibility has not been described to our knowledge. Therefore, the purpose of our study was the evaluation of the accuracy of flow velocity and volume measurement in a phantom study and to evaluate reproducibility when applied to the right coronary artery in healthy adult subjects while using a 3T breath-hold VE MRI sequence with spiral k-space sampling.

MATERIALS AND METHODS

Velocity-encoded MRI with spiral k-space sampling

All MRI studies were performed on a clinical 3T System (Achieva; Philips Medical Systems, Best, The Netherlands) using a six-element cardiac phased-array surface coil for signal reception. The accuracy of the VE MRI sequence was first tested in a phantom study (*in vitro*) with cardiac R-wave triggering simulation by using an artificial trigger pulse at a frequency of 1Hz. The reproducibility of the VE MRI sequence was subsequently tested *in vivo* by repeated acquisitions in 19 healthy adult human subjects. Each subject was placed in supine position and data were acquired using vector ECG triggering (10).

The VE MRI sequence used in the phantom-setup and in the healthy adult subjects was identical. Scan parameters were: repetition time (TR)=33ms, echo time (TE)=3.5ms, flip angle (FA)=20°, field-of-view (FOV)=250×250 mm^2, acquired spatial resolution 0.8×0.8×8mm^3, reconstructed spatial resolution 0.7×0.7×8.0 mm^3, spiral acquisition window 26ms, spiral interleaves 12, prospective ECG-triggering. Thirty flow encoded cine frames were acquired per second. One spiral interleave was acquired per cine frame and per heartbeat and data acquisition was completed in 24 flow compensated and flow encoded alternate cardiac cycles. To minimize the effects of off-resonance, ECG triggered shimming and a 1-2-1 spectral spatial water excitation for fat signal suppression were used (11).

In vitro testing of accuracy

In a phantom set-up, five constant flow rates (ranging from 0.9ml/s to 4.2ml/s) were applied to a straight tube of polyolefin with a luminal diameter of 4.4 mm, resulting in flow velocity values comparable to the expected *in vivo* coronary flow velocity values. The tube was positioned inside a water container. The flowing water through the tube was doped with gadolinium to shorten T1 of the fluid to approximately 100ms. VE MRI was performed perpendicular to the tube. The velocity sensitivity (V_{enc}) was adjusted for each acquisition according to the expected maximum velocity, and ranged from 15cm/s to 80cm/s. From the VE MRI, the flow rate was determined and compared with volumetric collection distal to the phantom in order to study the accuracy.

Flow velocity analysis was performed using the previously validated in-house developed software package FLOW (12). Manual region-of-interest (ROI) definition in the *in vitro* experiments was performed in two ways. A non-constricted ROI (i.e. approximately circular ROIs with mean area of 26.3mm^2; this covers all complete voxels that include at least part of the flowing water in the tube) was placed on the tube cross-section in the phase image in the first phase, segmenting all visible luminal velocity value s. Secondly, a constricted circular ROI with a fixed area of 15.3 mm^2 equal to the true dimension of the tubular lumen (i.e. the ground truth) was placed in the center of the tube cross-section. Both in the non-constricted and constricted ROIs, only voxels that show signs of phase dispersion (13) (i.e. voxels partially inside the wall presenting with random phase/velocity values) were removed from the analysis since they typically present with high positive or negative velocity and therefore can have a high negative contribution to flow analysis. These voxels are easy to identify and typically one or two voxels per image show phase dispersion.

The ROI was then copied to all the subsequent cine frames. The mean cross-sectional flow velocity was determined for each of these frames. Background correction (i.e. to correct for local phase offset errors (14)) was performed by measuring the mean velocity in a ROI in the background (i.e. in the surrounding water near the phantom). The flow rate was determined by multiplying the mean cross-sectional flow velocity after background subtraction with the cross-sectional area. Flow rate was determined for both constricted and non-constructed ROIs in the phantom.

In vivo testing of reproducibility

Nineteen healthy adult subjects (11 men, 8 women; mean age 25.4 ± 1.2 years) without a prior history of cardiovascular disease were included to evaluate the reproducibility of a breath-hold VE MRI-protocol to assess flow velocity in the RCA. All subjects gave written informed consent and local medical ethics committee approval was obtained. The VE MRI sequence was repeated in every healthy subject after repositioning. Subjects were removed from the MRI table and the complete procedure was repeated. Between examinations, the surface coil was removed. Reproducibility was tested by comparing indices extracted from both resulting RCA flow velocity-time graphs.

The first steps of our MRI plan scanning procedure for assessment of coronary artery flow velocity and volume were determined analogously to a study by Stuber et al. (15). Figure 1 demonstrates the localization steps of the MR imaging protocol. In short, a prospective ECG gated gradient-echo cine sequence with maximum velocity encoding perpendicular to a straight proximal vessel segment to the RCA close to the origin of the RCA was performed. The imaging plane was determined from a double-oblique-sagittal view of the RCA (Figure 1 middle image). This view of the RCA survey was localized by defining three points (three-points-plan-scan-tool) in the center of the RCA in a 3D volume of the heart which included the coronary arteries (Figure 1, top images) (15). Maximum velocity-encoding (V_{enc}) of 35

cm/s was used and in case of aliasing, the acquisition was repeated with an adjusted V_{enc} of 45–55 cm/s if needed.

In vivo flow velocity analysis was again performed using the previously validated in-house developed software package FLOW (12). To be able to better delineate the contours of the RCA also during periods of low coronary flow, manual ROI segmentation was defined for each of the cine frames using the information of both the magnitude and phase (i.e., velocity) images. Within the ROIs, the maximum cross-sectional flow velocity as well as the mean cross-sectional flow velocity were determined for each frame. Background correction (i.e. to correct both for local phase offset errors (14) as well as through-plane motion (3;16;17)was performed by using the mean velocity assessed in a ROI in the background tissue (i.e. in the lateral right ventricular wall near the cross-section of the RCA (mean area of this ROI was 13.1 ± 2.3 mm^2). Figure 2 demonstrates a zoomed magnitude and velocity image with the RCA and background ROIs at selected time points in the cardiac cycle (i.e. time = 0ms; time of most rapid contraction, i.e. end systole; time of most rapid expansion, i.e. late diastole) as an example of image segmentation.

Flow velocity-time graphs were determined by subtracting the background velocity from the maximum cross-sectional flow velocity determined throughout the cardiac cycle and subsequently plotted against time. Flow volume was determined by multiplying the mean cross-sectional velocities after background subtraction with the cross-sectional area, and furthermore by integrating these flow rate values over the cardiac cycle.

An example of an acquired coronary flow velocity-time graphis shown in Figure 3. From the corresponding *in vivo* data, the following indices were determined: peak systolic and diastolic velocity (PSV and PDV) (in cm/s), the maximum velocity from a single voxel within the defined ROI was determined for each phase and averaged over the cardiac cycle resulting in the mean maximum velocity (meanV_{max}) (in cm/s), ratio of PSV and PDV to meanV_{max} (indicating the pulsatility of V_{max}-pattern) and the ratio between peak systolic and diastolic velocity (PSV/PDV).

Together with the coronary flow volume per cardiac cycle (in ml), these indices were used for comparison between repeated acquisitions.

Manualcontour segmentation was performed by observer one with two years of experience in cardiacMR imaging. Segmentation of each VE MRI acquisition took 10–15 minutes. In a blinded manner,the same observer compared the repeated breath-hold VE MR images with the first VE MR images obtained in the RCA. Intra- and inter-observer variation of the image-processing procedure were also tested with repeated analysis by two observers in a blinded manner with two and fifteen years of experience with cardiac MR imaging, respectively and with an inter-examination time of more than one day.

Statistics

Continuous data are expressed as means ± 1 standard deviation (SD). Correlation between MRI flow rate measurements and volumetric collection distal to the phantom was evaluated with the Pearson correlation coefficient (r). The approach described by Bland and Altman was used to study systematic differences (18). In the repeated acquisitions in healthy adult subjects, mean signed differences, SD and 95 % confidence intervals (i.e. the limits of agreement) were determined and the difference between the repeated measurements was tested by using the paired-sampled t-tests with $p<0.05$ considered statistically significant. The intraclass correlation coefficient (ICC) for absolute agreement was calculated to assess interscan and intra-observer/inter-observer agreement, and the coefficient of variance (COV)

was determined. The COV was defined as the SD of the differences between the two series of measurements divided by the mean of both measurements.

RESULTS

In vitro

The results for the *in vitro* part of the study are presented in Figure 4. Although the correlation between VE MRI and volumetric collection is very strong (i.e. non-constricted ROIs r=0.99, p<0.01, constricted ROIs r= 0.998), p<0.01, the non-constricted ROI segmentation shows a statistically significant (p<0.01) overestimation in flow rate (i.e. mean bias = 0.92 ± 0.23 ml/s) as compared to volumetric collection distal to the phantom. This overestimation in mean flow rate is 47% ± 20% (mean error) but can amount up to 81% in selected cases.

Using the constricted ROI segmentation that includes a priori knowledge of the tube size, the flow rate assessment is accurate within 13% of the applied flow rates between 0.9ml/s and 4.2ml/s and no significant bias with the volumetric collection was found. Bland-Altman analysis shows that flow rate measurements for low flow rates (<2ml/s) are equal to the volumetric collection, but for higher flow rates (>2ml/s), flow volumes assessed with VE MRI are lower than the volumetric collection (Figure 4B). When using constricted ROIs, there is only a weak bias, and the error in flow rate assessed with VE MRI slowly increases with higher flow rates.

In vivo testing of reproducibility

From the 38 acquisitions in 19 healthy adult subjects, 7 acquisitions were unsuccessful (18%) because of poor image quality (i.e. mainly caused by ECG-triggering problems and/or inadequate breath holding). Therefore, four adult subjects were excluded for further analyses because of the unsuccessful acquisition(s). The range in breath-hold time was 15 to 23s. In the remaining 15 healthy adult subjects, the flow velocity measurements in the RCA were successfully repeated as shown in Table 1.

The mean difference between the repeated acquisitions was not significant for any of the indices describing the velocity-time graphs. Good to excellent agreement was found between the repeated acquisitions as all ICCs were significant for flow velocity indices and the flow volume, except for PDV/meanV_{max}. ICCs concerning interscan reproducibility were highest for PSV and PSV/meanV_{max} as well as for flow volume (0.88, 0.86, and 0.89, respectively). The COV of PSV and PSV/meanV_{max} and flow volume were 16%, 12%, and 24%, respectively. Bland-Altman plots of PSV, PDV, meanV_{max}, PSV/meanV_{max}, PSV/PDV, and flow volume for the repeated measures are given in Figure 5.

Table 2 presents the results of the intra-observer analysis. The mean difference for meanV_{max} between the repeated analysis was small but statistically significant (−0.5 cm/s, 95% CI −0.8 to −0.1 and p=0.01). All other indices showed no significant differences. ICCs concerning intra-observer variability were high for all flow velocity indices and flow volume. COVs for PDV and flow volume was 11%, for PSV and meanV_{max} only 4%.

In Table 3, the results of the inter-observer variability are listed. The mean difference between the repeated acquisitions was only statistically significant for PDV and flow volume (PDV: mean difference −1.2 cm/s; 95% CI −2.2 to −0.2 and p=0.02; Flow volume: 1.5 ml/cycle; 95% CI 0.3 to 2.7 and p=0.02). ICCs concerning inter-observer variability were highest for PSV, PDV, meanV_{max}, PSV/meanV_{max}, PDV/meanV_{max} and flow volume (0.98, 0.98, 0.94, 0.99, 0.96, and 0.94 respectively). COVs for PSV, PDV and meanV_{max} were less than 8% and COV for flow volume was less than 14%.

DISCUSSION

The main findings of the current study are as follows: first, in a phantom study, velocity-encoding with spiral k-space sampling at 3T proves to be accurate within 13% of the nominal flow rates between 0.9ml/s and 4.2ml/s when the true luminal area can accurately be traced. Second, *in vitro* VE MRI with spiral k-space sampling shows a mean overestimation of 47% in flow volume when non-constricted ROI segmentation on the phase-contrast images is used. Third, spiral k-space sampled breath-hold VE MRI can reproducibly assess flow velocity indices in the right coronary artery with a success rate of 82% in healthy adult subjects, while intra- and inter-observer variations are low.

Many authors have already described the accuracy of measuring volume flow in phantoms and in dogs using VE MRI with linear k-space sampling (19–23). In these reports, spatial resolution was mentioned as the main determinant of accuracy. Johnson et al. described the accuracy of flow assessment with VE MRI in small diameter vessels at 3T(5). Their *in vitro* phantom study demonstrated a root mean square error of 15% for VE MRI and relied on a VE MR FLASH sequence with segmented k-space sampling and an in-plane resolution of 1.0×1.0 mm (5). Keegan et al. demonstrated that the use of VE MRI with spiral k-space sampling for the assessment of coronary flow velocity with an in-plane resolution of 0.8×0.8mm is superior in accuracy when compared to a segmented FLASH sequence (7). Interleaved spiral phase contrast imaging has a smaller acquisition window and improved spatial and temporal resolution (7;9). However, their study relied on a 1.5T MRI system for *in vivo* evaluation of coronary flow and neither accuracy nor reproducibility were reported (7).

With VE MRI, both flow volume and flow velocity indices can be derived from the velocity-time graph. In our *in vitro* study, however, it was found that the appearance of the cross-sectional lumen on the phase-contrast images was on average 73% larger than the true lumen size and on the gradient-echo magnitude images, probably due to the limited spatial resolution (0.8×0.8mm voxel size for a 4.4mm diameter tube), which is in accordance with previous studies (19;21–23). Consequently, flow rate assessment using non-constricted ROI segmentation was systematically overestimated. When using constricted ROI segmentation with luminal area equal to the ground truth, no bias in flow volume assessment was found, suggesting that the velocity measurements are more accurate. This also implies that for *in vivo* measurements, if the ground truth of the cross-sectional luminal area is unknown and if the lumen cannot accurately be determined on the magnitude images, segmentation that relies on the velocity images only will lead to an overestimation in flow volume. However, in contrast to flow rate, flow volume and the mean flow velocity, the maximum flow velocity can still accurately be measured by non-constricted ROI segmentation on the velocity images.

The inter-scan reproducibility of coronary flow velocity assessment with VE MRI using spiral k-space sampling in asymptomatic healthy adult subjects was previously demonstrated on a 0.5T MRI system (8). However, the use of a 3T MRI system offers potentially higher signal-to-noise ratio as a result of the stronger B_0, which can be traded for a higher spatial and temporal resolution (24,25). In our study, higher in-plane resolution (i.e. 0.8×0.8mm versus 1.1×1.1 mm) and temporal resolution (i.e. 33ms versus 80–100ms (8)) were achieved, which is mandatory for adequate assessment of the indices describing the pulsatile flow velocity-time graph in the small and constantly moving coronary arteries.

We found that the indices of the flow velocity-time graph can be determined with high reproducibility in healthy adult subjects at 3T as all ICCs were significant for all parameters describing the velocity-time graph, except the PDV/meanV_{max}. However, the statistically

significant differences in the flow velocity indices found in the repeated analyses (i.e. in intra-observer study meanV_{max}, inter-observer study PDV and flow volume) are relatively small but have to be considered for future patient studies.

Mean flow velocity and flow volume may also be used as outcome parameters in coronary flow analyses. However, as described in the *in vitro* validation, both parameters depend on the ability to segment the cross-sectional luminal area of the coronary artery accurately. Therefore, we used the maximum cross-sectional flow velocity to determine reproducibility in the right coronary artery. An additional benefit is that maximum cross-sectional flow velocity assessment is less time consuming (26). Further, in clinical research studies, MRI peak flow velocities measured at rest and during dipyridamole stress are often used for calculating coronary flow velocity reserve to estimate the hemodynamic implication of a coronary artery stenosis (3). To support this, accurate and reproducible assessment of maximum cross-sectional flow velocity with MRI is mandatory and is supported by 3T spiral coronary flow measurements.

Our study has some limitations. First, 3T VE MRI with spiral k-space sampling was only performed in the right coronary artery in healthy adult subjects. The application of spiral VE MRI distal to stenotic lesions may be particularly promising as changes in the measured flow-velocity time graph can be expected. Accordingly, further studies in patients with advanced atherosclerosis are needed to verify the robustness of this MRI protocol. Furthermore, the accuracy in pulsatile flow measurements using a VE MR sequence with spiral k-space sampling at 3T MRI, remains to be explored. The use of prospective triggering is also a limitation. Data during the complete cardiac cycle are not obtained. The first frame for all scans was consistently acquired at 8 msec after the R-wave of the ECG but part of diastole was missing. This results in an underestimation in flow volume. However, assessment of the peak systolic and diastolic velocities remains unaffected. Furthermore, in this study we used a breath-hold VE MR approach to suppress respiratory motion. Other studies have shown that the use of a navigator-gated free-breathing acquisition improves accuracy of flow velocity assessment since the improved temporal resolution enables better assessment of peak flow velocity as compared to breath-holding (7). In our study, the suppression of respiratory motion was obtained by breath-holding in order to keep the total examination time short, as repeated measurements were needed to study reproducibility. However, a short scan duration supports the integration of coronary flow measurements at rest and during stress into a clinical cardiac exam.

In conclusion, 3T breath-hold VE MRI with spiral k-space sampling enables accurate and reproducible assessment of right coronary artery flow velocity with high spatial and temporal resolution. Although the correlation between *in vitro* flow rate assessment from VE MRI and volumetric collection was very strong, a significant 47% overestimation in flow volume may be expected if the ROI size cannot be determined from the modulus images. Segmentation with contours constricted to the true lumen diameter results in accurate flow volume and flow velocity assessment. Therefore flow volume assessment can be unreliable when the cross-sectional lumen is overestimated, but flow velocity measurements still remain accurate. Furthermore, in healthy adult subjects, right coronary artery flow velocity assessment with spiral VE MRI was successful in 82% of the cases. Although high intra- and inter-scan reproducibility was identified for almost all indices describing coronary flow velocity, measurement of peak systolic coronary flow velocity seems to be a particularly promising quantitative index and investigations of coronary flow in patients and distal to hemodynamically significant stenoses are now warranted.

Acknowledgments

Grant Support: Matthias Stuber and Robert G. Weiss are supported in part by the National Institutes of Health; Grant number: R01-HL084186 and by the D.W. Reynolds Foundation.

References

1. Napoli C, Lerman LO, de NF, Gossl M, Balestrieri ML, Lerman A. Rethinking primary prevention of atherosclerosis-related diseases. Circulation. 2006; 114(23):2517–2527. [PubMed: 17146003]
2. Gould KL, Lipscomb K, Hamilton GW. Physiologic basis for assessing critical coronary stenosis. Instantaneous flow response and regional distribution during coronary hyperemia as measures of coronary flow reserve. Am J Cardiol. 1974; 33(1):87–94. [PubMed: 4808557]
3. Sakuma H, Kawada N, Takeda K, Higgins CB. MR measurement of coronary blood flow. J Magn Reson Imaging. 1999; 10(5):728–733. [PubMed: 10548782]
4. Bluemke DA, Achenbach S, Budoff M, et al. Noninvasive coronary artery imaging: magnetic resonance angiography and multidetector computed tomography angiography: a scientific statement from the American heart association committee on cardiovascular imaging and intervention of the council on cardiovascular radiology and intervention, and the councils on clinical cardiology and cardiovascular disease in the young. Circulation. 2008; 118(5):586–606. [PubMed: 18586979]
5. Johnson K, Sharma P, Oshinski J. Coronary artery flow measurement using navigator echo gated phase contrast magnetic resonance velocity mapping at 3.0 T. J Biomech. 2008; 41(3):595–602. [PubMed: 18036532]
6. Gutberlet M, Spors B, Grothoff M, et al. Comparison of different cardiac MRI sequences at 1.5 T/3.0 T with respect to signal-to-noise and contrast-to-noise ratios - initial experience. Rofo. 2004; 176(6):801–808. [PubMed: 15173972]
7. Keegan J, Gatehouse PD, Mohiaddin RH, Yang GZ, Firmin DN. Comparison of spiral and FLASH phase velocity mapping, with and without breath-holding, for the assessment of left and right coronary artery blood flow velocity. J Magn Reson Imaging. 2004; 19(1):40–49. [PubMed: 14696219]
8. Keegan J, Gatehouse P, Yang GZ, Firmin D. Interleaved spiral cine coronary artery velocity mapping. Magn Reson Med. 2000; 43(6):787–792. [PubMed: 10861871]
9. Gatehouse PD, Keegan J, Crowe LA, et al. Applications of phase-contrast flow and velocity imaging in cardiovascular MRI. Eur Radiol. 2005; 15(10):2172–2184. [PubMed: 16003509]
10. Fischer SE, Wickline SA, Lorenz CH. Novel real-time R-wave detection algorithm based on the vectorcardiogram for accurate gated magnetic resonance acquisitions. Magn Reson Med. 1999; 42(2):361–370. [PubMed: 10440961]
11. Meyer CH, Pauly JM, Macovski A, Nishimura DG. Simultaneous spatial and spectral selective excitation. Magn Reson Med. 1990; 15(2):287–304. [PubMed: 2392053]
12. van der Geest RJ, Niezen RA, Van der Wall EE, de Roos A, Reiber JH. Automated measurement of volume flow in the ascending aorta using MR velocity maps: evaluation of inter- and intraobserver variability in healthy volunteers. J Comput Assist Tomogr. 1998; 22(6):904–911. [PubMed: 9843231]
13. Kilner PJ, Gatehouse PD, Firmin DN. Flow measurement by magnetic resonance: a unique asset worth optimising. J Cardiovasc Magn Reson. 2007; 9(4):723–728. [PubMed: 17613655]
14. Chernobelsky A, Shubayev O, Comeau CR, Wolff SD. Baseline correction of phase contrast images improves quantification of blood flow in the great vessels. J Cardiovasc Magn Reson. 2007; 9(4):681–685. [PubMed: 17578724]
15. Stuber M, Botnar RM, Danias PG, et al. Double-oblique free-breathing high resolution three-dimensional coronary magnetic resonance angiography. J Am Coll Cardiol. 1999; 34(2):524–531. [PubMed: 10440168]
16. Keegan J, Gatehouse PD, Yang GZ, Firmin DN. Spiral phase velocity mapping of left and right coronary artery blood flow: correction for through-plane motion using selective fat-only excitation. J Magn Reson Imaging. 2004; 20(6):953–960. [PubMed: 15558551]

17. Westenberg JJ, Roes SD, Ajmone MN, et al. Mitral valve and tricuspid valve blood flow: accurate quantification with 3D velocity-encoded MR imaging with retrospective valve tracking. Radiology. 2008; 249(3):792–800. [PubMed: 18849503]

18. Bland JM, Altman DG. Statistical methods for assessing agreement between two methods of clinical measurement. Lancet. 1986; 1(8476):307–310. [PubMed: 2868172]

19. Tang C, Blatter DD, Parker DL. Accuracy of phase-contrast flow measurements in the presence of partial-volume effects. J Magn Reson Imaging. 1993; 3(2):377–385. [PubMed: 8448400]

20. Sondergaard L, Stahlberg F, Thomsen C, et al. Comparison between retrospective gating and ECG triggering in magnetic resonance velocity mapping. J Magn Reson Imaging. 1993; 11(4):533–537.

21. Wolf RL, Ehman RL, Riederer SJ, Rossman PJ. Analysis of systematic and random error in MR volumetric flow measurements. Magn Reson Med. 1993; 30(1):82–91. [PubMed: 8371679]

22. Hofman MB, Visser FC, van Rossum AC, Vink QM, Sprenger M, Westerhof N. In vivo validation of magnetic resonance blood volume flow measurements with limited spatial resolution in small vessels. Magn Reson Med. 1995; 33(6):778–784. [PubMed: 7651113]

23. Arheden H, Saeed M, Tornqvist E, et al. Accuracy of segmented MR velocity mapping to measure small vessel pulsatile flow in a phantom simulating cardiac motion. J Magn Reson Imaging. 2001; 13(5):722–728. [PubMed: 11329193]

24. Wen H, Denison TJ, Singerman RW, Balaban RS. The intrinsic signal-to-noise ratio in human cardiac imaging at 1.5, 3, and 4 T. J Magn Reson. 1997; 125(1):65–71. [PubMed: 9245361]

25. Lotz J, Doker R, Noeske R, et al. In vitro validation of phase-contrast flow measurements at 3 T in comparison to 1.5 T: precision, accuracy, and signal-to-noise ratios. J Magn Reson Imaging. 2005; 21(5):604–610. [PubMed: 15834905]

26. Salm LP, Langerak SE, Vliegen HW, et al. Blood flow in coronary artery bypass vein grafts: volume versus velocity at cardiovascular MR imaging. Radiology. 2004; 232(3):915–920. [PubMed: 15273340]

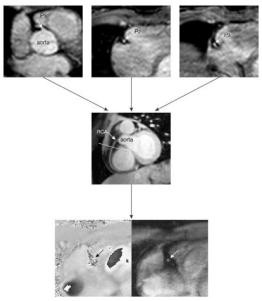

Figure 1.

Illustration of the scan protocol for assessing flow velocity in the right coronary artery (RCA)

The double-oblique-sagittal view of the RCA (4 in figure) was planned by defining three points (three-points-plan-scan tool) in the center of RCA on the images of the second scout scan (1, 2 and 3 in figure). The three points were subsequently chosen at the level of a proximal (1), a mid (2) and a more distal (3) segment of the RCA, respectively. The final breath-hold velocity-encoded (VE) MRI to assess coronary flow velocity in the RCA, was planned perpendicular to the RCA in a straight segment near to the origin of the RCA. The maximum number of phases was reconstructed during one average cardiac cycle. The bottom panels represent the phase and modulus image of one phase of the breath-hold VE MRI.

Figure 2.
Examples of contour definition on velocity and on magnitude images for right coronary artery flow assessment.
Top: represent t=0. Middle: represents time of most rapid contraction (end systole). Bottom: represents time of most rapid expansion (end diastole)

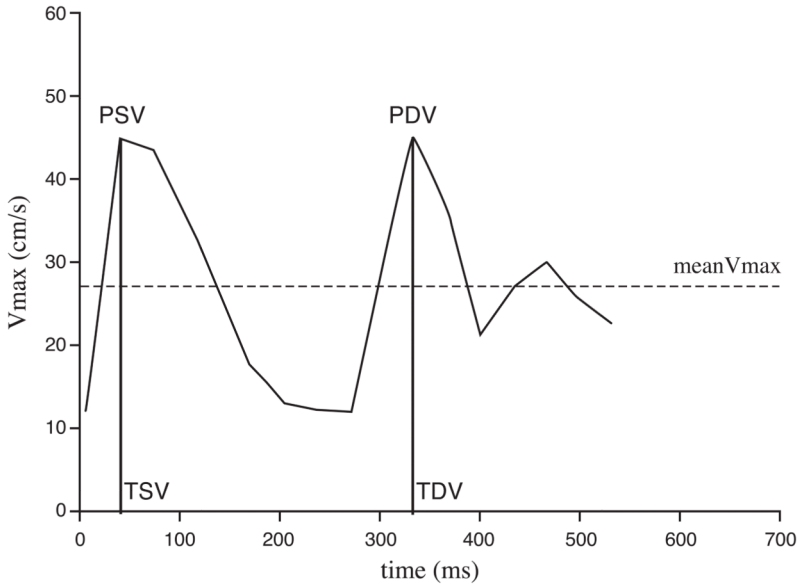

Figure 3.
Example of maximum velocity graph for RCA.
PSV: peak systolic velocity in cm/s; **TSV:** time of PSV in ms; **PDV:** peak diastolic velocity in cm/s; **TDV:** time of PDV in ms; **meanV$_{max}$**: maximum luminal velocity averaged over the cardiac cycle.

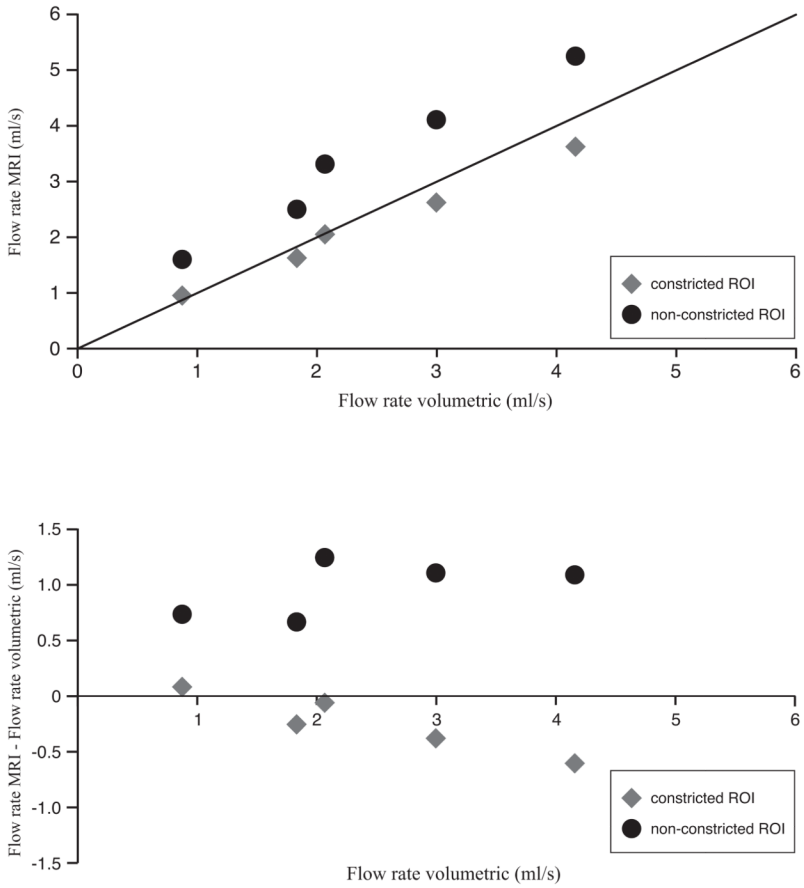

Figure 4.
Scatter diagram and Bland-Altman plot for *in vitro* flow volume validation.
Top: Flow rate was determined with VE MRI with spiral k-space sampling and compared with volumetric collection distal to the phantom. Bottom: Bland-Altman plot.

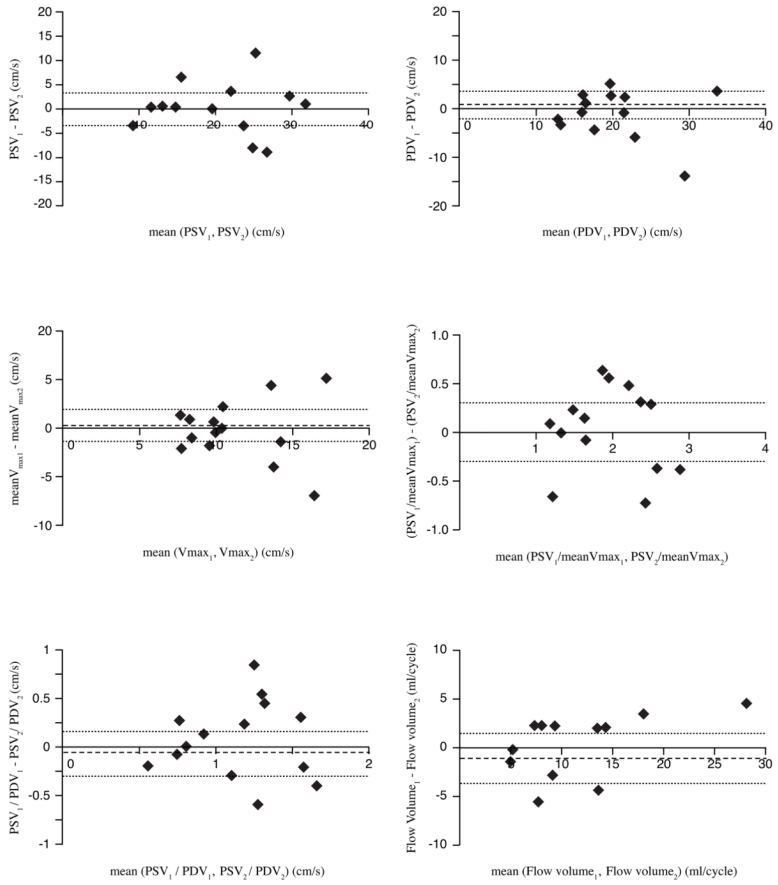

Figure 5.

Bland-Altman analysis for reproducibility of *in vivo* flow velocity and volume assessment: Top left: repeated assessment of PSV (peak systolic velocity); Top right: repeated assessment of PDV (peak diastolic velocity); Middle left: repeated assessment of meanV_{max} (maximum velocity within the defined ROI determined for each phase and averaged over the cardiac cycle); Middle right: repeated assessment of PSV/meanV_{max} (pulsatility of V_{max}-pattern); Bottom left: repeated assessment of PSV/PDV (peak systolic and diastolic velocity); Bottom right: repeated assessment of flow volume. Mean differences are presented as dotted lines, limits of agreement (95% confidence interval) are presented as dashed lines.

Table 1

Reproducibility of coronary artery flow velocity indices.

	Scan 1	*Scan 2*	*Paired t-test*			*Correlation*		
	mean ± sd	**mean ± sd**	**Mean difference**	**95% CI**	**p-value**	**ICC**	**p-value**	**COV(%)**
PSV (cm/s)	22.1 ± 8.4	21.8 ± 7.9	−0.0	−3.3 to 3.3	0.99	0.88*	(p < 0.01)	16
TSV (ms)	65 ± 15	65 ± 16	0.0	−7.5 to 7.5	1.00	0.80*	(p < 0.01)	19
PDV (cm/s)	19.8 ± 6.8	19.1 ± 6.3	1.1	−1.8 to 3.9	0.44	0.84*	(p < 0.01)	17
TDV (ms)	387 ± 51	404 ± 72	−20.2	−44.5 to 4.1	0.10	0.85*	(p < 0.01)	9
$meanV_{max}$ (cm/s)	11.3 ± 3.5	11.2 ± 3.5	0.2	−1.6 to 2.0	0.84	0.77*	(p < 0.01)	18
$PSV/meanV_{max}$	2.0 ± 0.6	2.0 ± 0.6	−0.0	−0.3 to 0.2	0.71	0.86*	(p < 0.01)	12
$PDV/meanV_{max}$	1.8 ± 0.4	1.7 ± 0.3	0.1	−0.2 to 0.4	0.48	0.22	(p = 0.34)	16
PSV/PDV	1.2 ± 0.4	1.2 ± 0.4	−0.1	−0.3 to 0.2	0.49	0.67*	(p = 0.03)	20
Flow volume (ml/cycle)	11.4 ± 5.4	12.5 ± 7.9	−1.0	−3.6 to 1.5	0.39	0.89*	(p < 0.01)	24

PSV: peak systolic velocity in cm/s; TSV: time of PSV in ms; PDV: peak diastolic velocity in cm/s; TDV: time of PDV in ms; $meanV_{max}$: maximal velocity averaged over the cardiac cycle; $PSV/meanV_{max}$: measure for discriminating the systolic peak in the velocity-time graph; $PDV/meanV_{max}$: measure for discriminating the diastolic peak in the velocity-time graph; PSV/PDV: ratio between systolic and diastolic peak velocity; Flow volume: the total amount of coronary flow volume (ml/cycle).

*Mean and standard deviations (SD) are given for the flow velocity indices. Repeated acquisitions were compared using the paired *t*-test, mean difference, 95% confidence intervals (95% CIs) and p-values were given. The reproducibility of coronary flow assessment was evaluated using intraclass correlation coefficients (ICCs) for absolute agreement.

*p<0.05. Furthermore coefficients of variance (COVs) were given.

Table 2

Intra-observer analyses for the coronary artery flow velocity indices.

	Scan 1	*Scan 1*	*Paired t-test*			*Correlation*		
	mean ± sd	**mean ± sd**	**Mean difference**	**95% CI**	**p-value**	**ICC**	**p-value**	**COV(%)**
PSV (cm/s)	22.1 ± 8.4	22.5 ± 8.3	−0.4	−1.3 to 0.4	0.27	0.99*	(p < 0.01)	4
TSV (ms)	65 ± 15	65 ± 15	−0.9	−1.8 to 0.1	0.07	0.99*	(p < 0.01)	0
PDV (cm/s)	19.8 ± 6.8	20.2 ± 7.1	−0.5	−1.9 to 0.9	0.48	0.97*	(p < 0.01)	11
TDV (ms)	387 ± 51	391 ± 54	−0.4	−10.8 to 2.0	0.16	0.99*	(p < 0.01)	3
meanV$_{max}$ (cm/s)	11.3 ± 3.5	11.8 ± 3.4	−0.5	−0.8 to−0.1	0.01*	0.99*	(p < 0.01)	4
PSV/meanV$_{max}$	2.0 ± 0.6	1.9 ± 1.5	0.1	−0.0 to 0.1	0.12	0.99*	(p < 0.01)	5
PDV/meanV$_{max}$	1.8 ± 0.4	1.7 ± 0.5	0.0	−0.1 to 0.1	0.56	0.94*	(p < 0.01)	8
PSV/PDV	1.2 ± 0.4	1.2 ± 0.4	0.0	−0.1 to 0.1	0.97	0.97*	(p < 0.01)	9
Flow volume (ml/cycle)	11.4 ± 5.4	12.3 ± 6.4	−0.9	−1.8 to 0.1	0.07	0.97*	(p < 0.01)	11

PSV: peak systolic velocity in cm/s; TSV: time of PSV in ms; PDV: peak diastolic velocity in cm/s; TDV: time of PDV in ms; meanV$_{max}$: maximal velocity averaged over the cardiac cycle; PSV/meanV$_{max}$: measure for discriminating the systolic peak in the velocity-time graph; PDV/meanV$_{max}$: measure for discriminating the diastolic peak in the velocity-time graph; PSV/PDV: ratio between systolic and diastolic peak velocity; Flow volume: the total amount of coronary flow volume (ml/cycle).

*Mean and standard deviations (SD) are given for the flow velocity indices. Repeated analyses were compared using the paired *t*-test, mean difference, 95% confidence intervals (95% CIs) and p-values were given. Agreement between intra-observer analyses was evaluated using intraclass correlation coefficients (ICCs) for absolute agreement.

*p<0.05. Furthermore coefficients of variance (COVs) were given.

Table 3

Inter-observer analyses for coronary artery flow velocity indices.

	Scan 1	*Scan 1*	*Paired t-test*			*Correlation*		
	mean ± sd	**mean ± sd**	**Mean difference**	**95% CI**	**p-value**	**ICC**	**p-value**	**COV(%)**
PSV (cm/s)	22.1 ± 8.4	22.7 ± 10.3	−0.6	−2.2 to 1.0	0.42	0.98*	(p < 0.01)	8
TSV (ms)	65 ± 15	72 ± 26.4	−6.6	−16.9 to 3.7	0.19	0.76*	(p = 0.05)	27
PDV (cm/s)	19.8 ± 6.8	21.0 ± 6.8	−1.2	−2.2 to −0.2	0.02*	0.98*	(p < 0.01)	7
TDV (ms)	387 ± 51	398 ± 66	−10.9	−37.1 to 15.3	0.39	0.81*	(p < 0.01)	11
$meanV_{max}$ (cm/s)	11.3 ± 3.5	11.8 ± 3.8	−0.0	−0.4 to 0.3	0.81	0.94*	(p < 0.01)	3
$PSV/meanV_{max}$	2.0 ± 0.6	2.0 ± 0.7	0.0	−0.2 to 0.1	0.66	0.99*	(p < 0.01)	9
$PDV/meanV_{max}$	1.8 ± 0.4	1.9 ± 3.4	−0.1	−0.3 to 0.0	0.07	0.96*	(p < 0.01)	9
PSV/PDV	1.2 ± 0.5	1.1 ± 0.5	0.1	−0.1 to 0.2	0.27	0.88*	(p < 0.01)	12
Flow volume (ml/cycle)	11.4 ± 5.4	9.9 ± 5.1	1.5	0.3 to 2.7	0.02*	0.94*	(p < 0.01)	14

PSV: peak systolic velocity in cm/s; TSV: time of PSV in ms; PDV: peak diastolic velocity in cm/s; TDV: time of PDV in ms; $meanV_{max}$: maximal velocity averaged over the cardiac cycle; $PSV/meanV_{max}$: measure for discriminating the systolic peak in the velocity-time graph; $PDV/meanV_{max}$: measure for discriminating the diastolic peak in the velocity-time graph; PSV/PDV: ratio between systolic and diastolic peak velocity; Flow volume: the total amount of coronary flow volume (ml/cycle).

*Mean and standard deviations (SD) are given for the flow velocity indices. Analyses between observers were compared using the paired *t*-test, mean difference, 95% confidence intervals (95% CIs) and p-values were given. Agreement between observers was evaluated using intraclass correlation coefficients (ICCs) for absolute agreement.

*$p<0.05$. Furthermore coefficients of variance (COVs) were given.